Dear Author,

Please use this PDF proof to check the layout of your chapter. If you would like any changes to be made to the layout, you can leave instructions in the online proofing interface.

Making your changes directly in the online proofing interface is the quickest, easiest way to correct and submit your proof. Please note that changes made to the chapter in the online proofing interface will be added to the chapter before publication, but are not reflected in this PDF proof.

If you would prefer to submit your corrections by annotating the PDF proof, please download and submit an annotatable PDF proof by following this link:

http://rscbooksweb1.proofcentral.com/en/offline.html?token=f805db4fce1d0c5d6ae1e59c18c35418

AUTHOR QUERY FORM

Book Title: Quenched-phosphorescence Detection of Molecular Oxygen: Applications in Life Sciences
Chapter: 7

AQ1	Please check the word 'taylorize', should it be 'tailor' or 'Taylorize', or something else?
AQ2	A citation to Figure 7.3 has been added here, please check that the placement of this citation is suitable. If the location is not suitable, please indicate where in the text the citation should be inserted.
AQ3	The word 'intermitted' has been changed to 'intermittent', please check that this change is correct.
AQ4	The word 'neglectable' has been changed to 'negligible', please check that this is correct.
AQ5	Please clarify the meaning of '10th of cm^2'. Could this be changed to 'mm^2'?
AQ6	Please check that ref. 6 and 15 have been displayed correctly.
AQ7	Ref. 13: Please provide the year of publication.
AQ8	Ref. 38, 50, 52, 53, 103 and 107: Can these references be updated?
AQ9	Ref. 54: Please provide the year of publication and page (or article) number(s).

Abstract

Optical O_2 measurements with fiber-optic, planar or particle-based opt(r)odes have become widespread in aquatic science since the first O_2 microopt(r)odes were introduced in 1995. A wide variety of measuring systems are now available both for lab-based and *in situ* field measurements at spatial scales ranging from μm to m's, and temporal scales ranging from <1 s to several months. Furthermore, the market has seen an explosion in commercially available optical O_2 sensor and measuring systems, which complement or have replaced electrochemical O_2 sensors in several areas of application. In this chapter, we give a broad overview of measuring schemes and instruments used for optical O_2 sensing, and illustrate their application in various aquatic environments. We also address demands and challenges related to optical O_2 sensing in aquatic systems.

CHAPTER 7

Optical O_2 Sensing in Aquatic Systems and Organisms

KLAUS KOREN[a] AND MICHAEL KÜHL*[a,b]

[a]Marine Biological Section, Department of Biology, University of Copenhagen, Helsingør, DK-3000, Denmark; [b]Plant Functional Biology and Climate Change Cluster, University of Technology Sydney, Ultimo, New South Wales 2007, Australia
*E-mail: mkuhl@bio.ku.dk

7.1 Introduction

Molecular oxygen (O_2) is a key analyte in aquatic systems, where the balance is between: (i) production *via* oxygenic photosynthesis, (ii) consumption *via* aerobic respiration and re-oxidation of reduced chemical species, and (iii) transport *via* diffusion and advection controls the O_2 concentration. Measurements of net O_2 consumption/production are thus important proxies for primary production and carbon mineralization in aquatic habitats.[1] The solubility and diffusion of O_2 in water is relatively low, where the content of O_2 in 1 L air-saturated water is about 1/30 of the O_2 content in 1 L atmospheric air, and where the molecular diffusion coefficient of O_2 in water is about 10 000 times lower than in air.[2] As aquatic organisms, microbial cell aggregates, biofilms and impermeable sediments exchange solutes with the surrounding/overlaying water phase *via* a diffusive boundary layer (DBL),[3,4] the O_2 supply often becomes limiting in systems with high availability of organic matter leading to the formation of pronounced

Detection Science Series No. 11
Quenched-phosphorescence Detection of Molecular Oxygen: Applications in Life Sciences
Edited by Dmitri B. Papkovsky and Ruslan I. Dmitriev

Published by the Royal Society of Chemistry, www.rsc.org

O_2 concentration gradients. The quantification of O_2 concentration and dynamics is thus a key component of many ecophysiological and biogeochemical studies in freshwater and marine systems, and many measuring schemes have been applied. Historically, one of the most applied (and precise) methods for measuring O_2 is the well-established Winkler titration method.[5] While this method is sufficient to quantify bulk water O_2 levels, it requires sampling of relatively large volumes and has a limited time resolution, and the preferred method for measuring O_2 in aquatic samples now relies on the use of chemical O_2 sensors with high specificity, reversibility, and sensitivity.

Electrochemical O_2 sensors, and especially polarographic cathode-type and Clark-type O_2 electrodes,[6,7] have been the predominant O_2 sensors in aquatic science for many years, including the development of O_2 microelectrodes[8] and trace O_2 sensors,[9] which have changed our understanding of O_2 dynamics in biofilms, sediments, and the water column.[3,10–14] However, electrochemical O_2 sensors are now increasingly complemented or exchanged with luminescence quenching-based optical O_2 sensors, *i.e.* O_2 opt(r)odes, for aquatic analyses. Although the principle of luminescence quenching by O_2 has been known for a long time,[15] optical O_2 sensing was mostly used in blood gas analysis before it was introduced to aquatic science in 1995.[16] In the past 20 years, a variety of O_2 sensors have been developed and commercialized, and optodes have also enabled new measuring schemes and applications in terms of O_2 imaging, distributed sensing with sensor particles, and trace analysis.[16–22]

In this chapter, we review different optical O_2 sensor platforms and their application in aquatic science following a chronological as well as application-oriented order. Additionally, we highlight the demands and challenges related to O_2 sensing in aquatic systems.

7.2 Optical O_2 Sensing Platforms

All O_2 opt(r)ode sensor platforms rely on the same basic sensing mechanism, *i.e.*, collision-based quenching of an excited indicator dye embedded in a matrix (the so-called receptor). Collision-based dynamic quenching lowers both the luminescence intensity and decay time of the indicator. This quenching mechanism does not consume O_2 as the produced singlet oxygen can return to the ground state. In an ideal case, such quenching can be described by the Stern–Volmer relationship (eqn (7.1)) that relates the change in luminescence intensity (I) or decay time (τ) to the O_2 concentration:

$$\frac{I_0}{I} = \frac{\tau_0}{\tau} = 1 + K_{SV}[O_2], \tag{7.1}$$

where I_0 and τ_0 represent the luminescence intensity and decay time, respectively, in the absence of the quencher (O_2).

However, in practice an ideal Stern–Volmer relationship is not achieved with most sensors, where the immobilization of the indicator dye in a polymer matrix leads to the establishment of more quenchable and a less-quenchable fraction, which is often described by the so-called two-site model[23,24] (eqn (7.2)).

$$\frac{I}{I_0} = \frac{\tau}{\tau_0} = \frac{f_1}{1 + K_{SV}{}^1[O_2]} + \frac{f_2}{1 + K_{SV}{}^2[O_2]} \tag{7.2}$$

The factors f_1 and f_2 describe the percentage of indicator within the two fractions, and $K_{SV}{}^1$ and $K_{SV}{}^2$ denote the corresponding quenching coefficients. If one of the K_{SV} values is much higher than the other it is possible to set the lower value equal to zero, *i.e.*, introduce a non-quenchable fraction of the indicator. This simplifies the mathematical expression. Generally, it is important to describe the calibration function in detail and to determine the mentioned parameters in order to enable simple two-point calibration of the sensor. For two-point calibration, measurements in air-saturated and anoxic medium are typically employed. It is important to notice that temperature compensation is essential in order to obtain reliable O_2 measurements,[25] as temperature not only effects the O_2 solubility, but also the calibration of the sensor. Salinity has an additional effect on O_2 solubility and is thus relevant in marine applications.

The sensor sensitivity can be tuned by changing either the decay time of the indicator[26] or the O_2 permeability of the matrix.[27] Signal intensities can also be enhanced by adding scattering particles to the sensor layer, which enhances excitation efficiency and homogenizes the dye exposure and emission in the polymer matrix.[28,29] Further details on the basics of O_2 optode measuring schemes and characteristics can be found in recent reviews[25,26] and in other chapters of this book.

In order to enable optical O_2 measurements, the receptor needs to be excited and the obtained luminescence needs to be recorded. Excitation light as well as the obtained luminescence signal can be guided to the receptor and towards the detector unit (photodiode, photomultiplier or camera) by several means. Depending on the optical design of the light paths and the construction of the sensor, several sensing platforms can be distinguished. The most important sensing platforms for aquatic applications are briefly described in the following.

7.2.1 Fiber-optic O_2 Opt(r)odes

The probably most widely used sensor platform for optical O_2 sensing uses optical fibers to transport light towards and from the receptor. Total internal reflection within the optical fiber(s) transports excitation light from the light source to the receptor (indicator within polymer matrix) immobilized at the tip of the fiber, and the O_2-dependent luminescence is guided back to a detector. This setup is highly flexible and enables several measuring geometries.

While initially bulky instrumentation like spectrometers, lasers or large lamps[17] were used for excitation and readout purposes, rapid advancements in optoelectronic components have enabled significant miniaturization of the detection systems used with O_2 opt(r)odes. Nowadays, optoelectronic measuring systems for opt(r)odes are based on relatively cheap and low-power consuming components like light emitting diodes (LEDs) and photodiodes. In combination with advancements in electronics and battery technology, standalone instruments capable of long term *in situ* monitoring are now increasingly employed in aquatic science.

Fiber-optic opt(r)odes have the receptor immobilized on the analyte-exposed end of an optical fiber. Different types of immobilization are possible and chosen depending on the application. Measurements in "bulk" water are done with a large receptor area, which is often glued or screwed on to the tip of glass or plastic fiber (see Figure 7.1). This enables straightforward exchange of the receptor and uncouples the optics from the receptor. Such sensors normally have a sensor tip of 1–10 mm and find application in water monitoring or gas exchange measurements in respirometers or fermenters. They are mechanically robust and easy to handle.

In applications involving small sample volumes, measurements of O_2 concentration gradients or requiring fast response times, the glass fiber tip is miniaturized or tapered *e.g.* by chemical etching[30] or local heating.[31,32] Afterwards, the receptor (indicator and matrix dissolved in suitable solvent) is typically applied by dip coating. Sometimes, it is necessary to modify the glass surface prior to the coating process in order to increase adhesion.[33] Micro-opt(r)odes[16,18,34,35] are characterized by a small sensor tip of <0.1 mm (Figure 7.1). Very fast response times (<0.5–1 s) and high spatial resolution (<50 μm) can be obtained due to the small receptor volume at the measuring tip. Micro-opt(r)odes find application in for example profiling or eddy-correlation experiments.

Fiber-optic O_2 opt(r)odes can be regarded as the optical counterpart to the classical amperometric Clark-type electrodes that also can be manufactured for bulk water sensing or for microscale measurements.[8] In contrast to Clark-type sensors, optical sensors generally do not consume the analyte (see above) and do not display stirring sensitivity of the measuring signal. Additionally, fiber-optical opt(r)odes need less maintenance than electrolyte-containing electrodes and generally exhibit long-term stability in their calibration and other measuring characteristics. This makes opt(r)odes very attractive for long-term monitoring, and almost all commercial electrode/sensor providers have nowadays added O_2 opt(r)odes to their portfolio.

7.2.2 Planar Opt(r)odes for O_2 Imaging and Remote Read-out

A particular interesting sensing scheme for optical sensors is to use them for imaging chemical parameters using cameras as a detector. This enables 2D (or even 3D) measurements of O_2. Shortly after the first fiber-based

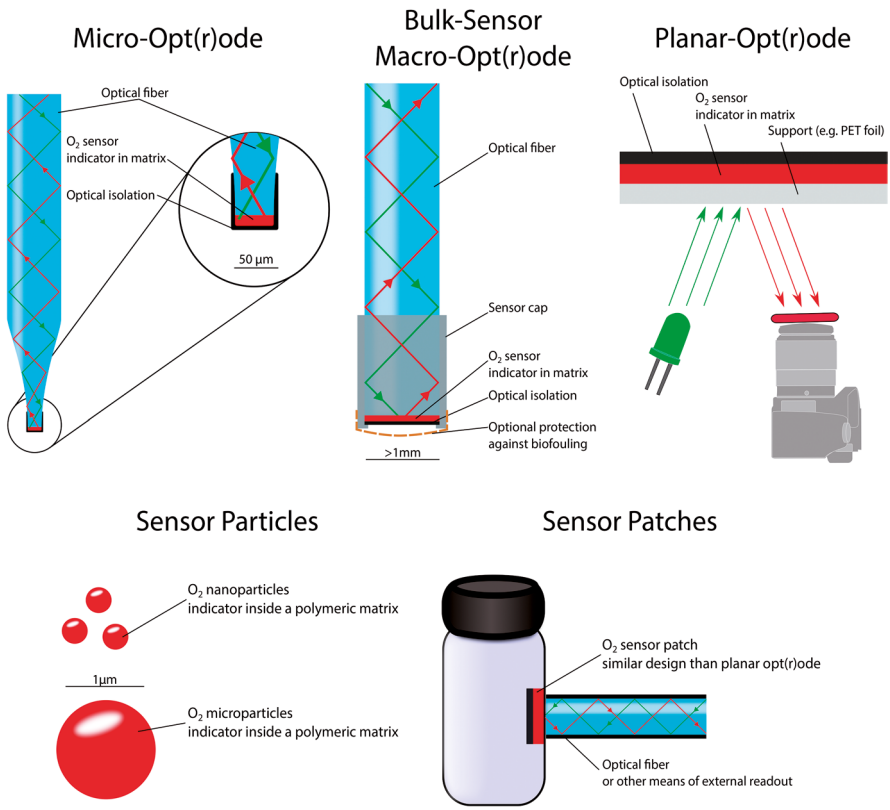

Figure 7.1 Commonly used sensor platforms for optical O_2 measurements in aquatic systems. Fiber-optic sensors are constructed either as micro-opt(r)odes or as macro-opt(r)odes. Micro-opt(r)odes enable high resolution O_2 measurements, while macro-opt(r)odes are more mechanically robust and typically used for longer term bulk measurements. Planar opt(r)odes enable chemical imaging using camera based read-out. Sensor nano- or microparticles can be dispersed within the sample or used to coat tissues, biofilms or other (a)biotic structures. By integrating a sensor patch (small piece of a planar opt(r)ode) within a vessel, the internal O_2 levels can be read out non-invasively through the transparent wall.

O_2 sensors were introduced[16] such 2D imaging setups were also developed for use in aquatic systems.[28,36] For 2D imaging, the receptor is immobilized on a transparent O_2 impermeable planar support (*e.g.* a glass cover slip or plastic polymer foil) (Figure 7.1). Large areas of such solid support can be covered with a homogeneous receptor layer by simple knife-coating[28,37] or spin-coating processes.[33] The planar support for the receptor can also be replaced by a fiber-optic faceplate in order to increase the spatial resolution of the sensor.[38] Such planar opt(r)odes can be put in contact with the sample *e.g.* by pressing a sample against the sensor foil,[28] inserting it into the sample *via* a periscopic

imaging system,[39] or by growing cells and biofilms on top of the sensor foil.[33] In all cases, the receptor is excited from behind (typically by LED's) through the transparent carrier, and the O_2-dependend luminescence distribution is imaged with a camera. First systems simply used the O_2-dependent change in luminescence intensity,[28] but have since been replaced by more robust decay time based[36,40] and ratiometric[41] imaging systems, which are less influenced by *e.g.* uneven illumination or indicator distribution.[42]

Imaging with planar opt(r)odes enables visualizing O_2 distribution on a larger scale, while still preserving high spatial and temporal resolution. The spatial resolution is determined by the imaged size compared to the resolution of the camera; *e.g.* 1 cm × 1 cm with 1000 × 1000 pixels results in a resolution of 10 μm per pixel. Several studies have used planar opt(r)odes to visualize O_2 hotspots in marine environments.[39,43,44] Despite their advantage of generating 2D data, planar optodes also have a few disadvantages for aquatic applications. Up front it has to be ensured that the sample is in good contact with the planar opt(r)ode, which often requires manipulation of the system and limits their application to sample surfaces with pronounced topography. The opt(r)ode itself acts as a diffusion barrier and will change the flow pattern at the surface, which can lead to unwanted "smearing" or "edge" effects.[28] Another type of smearing effect can occur when pushing planar optodes into samples.[39,45]

Also within this category, the so-called sensor patches should be mentioned. This means that small pieces of sensor foil (planar opt(r)ode) are fixed inside a transparent vessel, while sensor readout is facilitated *via* the transparent vessel wall by pointing a fiber at the sensor spot. Such patches can be integrated in all sorts of vessels such as fermenters or respirometry chambers, and readout can be realized with different optical emitter/detector units.[46]

7.2.3 Particle-based Optical O_2 Sensors

An imaging-based sensor platform that has been introduced to aquatic systems relatively recently[22] employs distributed sensing with micro- or nano-meter sized O_2 sensor particles. Rather than coating the receptor (indicator within a matrix) onto a fiber tip or a planar carrier, solid support particles can be made out of the matrix containing the indicator. Several straightforward methods for fabrication and use of O_2 sensitive particles are available.[47–50] Such sensor particles may also contain additional functionalities, like surface functionalization and magnetic properties,[47] making them attractive *e.g.* in applications mapping O_2 dynamics on flow-exposed surfaces that are coated with O_2 sensitive particles.[22,51] Sensor particles can also be immobilized into (semi)transparent gels such as agar and agarose, which can be used for embedding biological samples. This has *e.g.* been used for mapping the distribution and dynamics of O_2 in the rhizosphere of aquatic plants, which were planted in artificial sediments containing O_2 sensor particles.[20]

7.3 Challenges Related to Optical O_2 Measurements in Aquatic Systems

Aquatic habitats exhibit an extreme variety in environmental conditions, which present challenges to environmental O_2 monitoring. In polar or alpine regions, sensors have to deal with low temperatures, in the deep-sea extreme pressures prevail, and in light-exposed habitats strong solar radiation (including UV radiation) can lead to sensor bleaching and deterioration. Furthermore, several environmental parameters might change in parallel *e.g.* in intertidal zones, where temperature, salinity and light co-vary. In order to meet these and many other challenges, special sensor designs have been developed. Below, we discuss some of the common challenges and solutions for optical O_2 measurements in various aquatic systems.

7.3.1 Large O_2 Dynamics

While O_2 levels within certain environments and organisms are highly regulated (*e.g.* blood oxygenation), aquatic systems can exhibit extremely varying O_2 levels. Photosynthetic systems like microbial mats or dense algal cultures can easily reach O_2 levels exceeding air-saturation several times and approaching 100% O_2 when exposed to light.[16] At the other extreme, the so-called oxygen minimum zones (OMZ) in the oceans are characterized by extremely low O_2 availability in the nM range.[52–54] An advantage of optical O_2 sensors is that they can relatively easily be optimized for specific measuring characteristics needed in a particular habitat without changing the basic optical readout methods.

The dynamic range of an optical O_2 sensor can be tuned by altering the decay time of the indicator or the permeability of the immobilization polymer matrix. Due to intense research on indicator synthesis, many different classes and variants of indicators are described[25,26] and can be used to AQ1 taylorize the measuring characteristics of O_2 opt(r)odes. Additionally, the permeability of the polymer can be altered by either changing the type of polymer[25] or by altering the monomer structure.[27] The latter may be the preferred method when only slight (2–5 times) changes in sensitivity are desirable. Changing to an entirely different polymer (*e.g.* between less permeable polystyrene and highly permeable silicone) can result in more dramatic changes in the sensitivity, but one has to be careful that the indicator and the polymer are compatible. If the indicator does not dissolve well in the polymer or even aggregates within the polymer, this leads to signal drift and changing sensor calibration.

Many commercial providers of O_2 opt(r)odes (*e.g.* Pyro-Science GmbH, Presens GmbH, Ocean Optics) offer sensors optimized for different dynamic ranges, *i.e.*, normal range O_2 sensors (typically 0–50% O_2 with a limit of detection (LOD) of 0.02% O_2) and trace O_2 sensors (typically 0–10% O_2 with LOD of 0.005% O_2). Commonly used oceanographic sensors have an LOD of ~1 μM, which is generally acceptable. However, in oxygen minimum zones (OMZs)

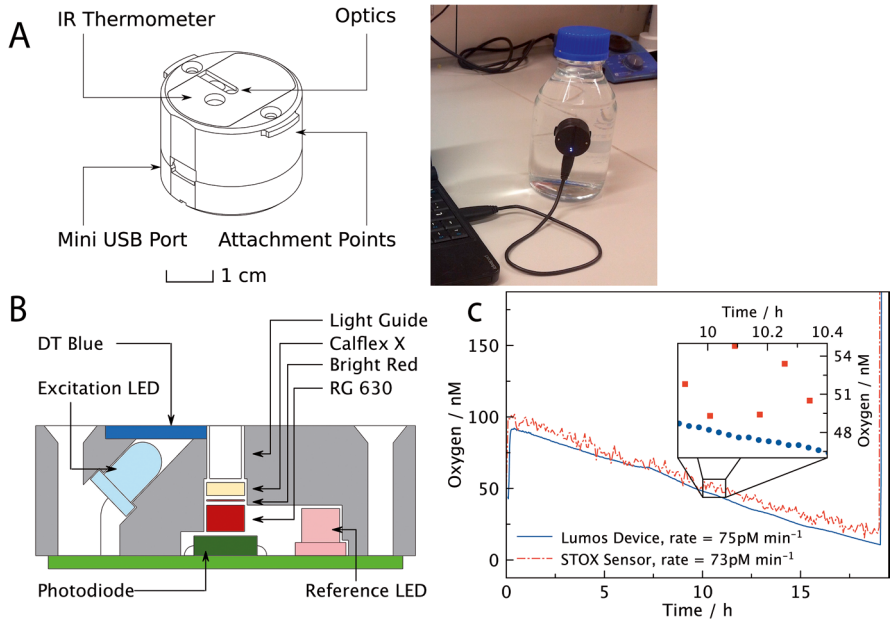

Figure 7.2 Design and application of the LUMOS[46] sensor device for trace O_2 measurements (A). The entire optics (panel B), an IR thermometer and the electronic components are packed into a small device that can be attached to a vessel containing the trace O_2 sensor patch. The optical trace sensor provides similar respiration rates than an electrochemical trace O_2 sensor (STOX), but the LUMOS data is less noisy (C). Reprinted from *PLoS One*, 2015, **10**, e0128125,[46] https://doi.org/10.1371/journal.pone.0128125. © 2015 Lehner *et al.* Published under a CC BY 4.0 licence, https://creativecommons.org/licenses/by/4.0/.

a significantly lower LOD is needed to describe the true O_2 availability. Therefore, highly sensitive trace O_2 opt(r)odes were developed.[46,55] Larsen *et al.* (2016) used a combination of a standard (LOD 200 nM), a mid-range (LOD 50 nM) and a trace sensor (LOD 5 nM) in order to fully describe the O_2 profile within an OMZ.[55] Also, O_2 consumption measurements at nM concentrations were performed using a specially developed sensor material and optical setup (LUMOS)[46,56] (see Figure 7.2). Optical sensors for ultra-trace O_2 measurements enable O_2 measurements down to a LOD of 7 pM.[57] Optical O_2 sensors thus outcompete electrochemical sensors in terms of LOD; although also highly sensitive trace electrochemical O_2 sensors were developed and successfully applied.[9,58]

7.3.2 Extreme Environments Require Special Designs

As mentioned, extreme conditions can be found within aquatic habitats. Probably some of the harshest environments on Earth are found in the deep marine trenches under extreme hydrostatic pressure and low temperature.

Nevertheless, optical O_2 sensors have also been applied successfully in such extreme deep-sea habitats. First, micro-opt(r)odes were adopted and tested for use at high pressures,[59] showing that the performance of O_2 micro-opt(r)odes is similar to pressure-compensated O_2 microelectrodes. Also 2D imaging setups have been developed and tested for imaging O_2 in the seafloor[39,44] both in coastal regions[39] and the deep sea.[44] This enabled *in situ* visualization of the spatio-temporal O_2 dynamics in the seafloor as affected by worm burrows and other animal activities (bioturbation and bio-irrigation),[60] sedimentation of marine snow particles, as well as photosynthetic O_2 production in shallow waters.[39,61]

Besides extreme hydrostatic pressure, also extreme temperatures can be challenging for optical O_2 sensors. Besides the need to apply the appropriate corrections for temperature and salinity effects, opt(r)odes are well suited for measurements below 0 °C as the sensor does not contain any electrolyte or other liquid phases that could freeze; this can be a problem for electrode-based sensors. Microopt(r)odes have for example been applied within sea ice, where sensors have either been frozen into forming sea ice[62] or used to measure gradients at the sea ice water interface.[63] Also planar opt(r)odes have been used at temperatures below 0 °C to investigate the O_2 dynamics in sea ice during melting.[64]

O_2 opt(r)odes are also well suited for measurements in hot water. Many commercial sensors are specified for measurements in water up to 55 °C, but as long as the mechanical properties of the sensor matrix are not affected, measurements at much higher temperatures are possible *e.g.* in geothermal springs where microopt(r)odes have been applied up to 85 °C (M. Kühl, unpublished data).

A further challenge for optical O_2 sensors arises from background irradiance. When measuring O_2 production within photosynthetic systems such as microbial mats, biofilms or a coral reef, the sensor may be exposed to high levels of solar radiation including high levels of UV light. This can lead to bleaching of the indicator and saturation of the detector by background light (despite strong spectral filtering). Solutions for this include the use of an O_2 permeable optical isolation layer on microopt(r)odes[16] or planar sensors,[65] which may however result in a longer response time. Nevertheless, it remains important to check that the background light is not affecting the measurement. Background light can be better controlled in the laboratory, and it might also be possible and useful to switch the light source (*e.g.* used to stimulate photosynthesis) off, *e.g.* at the onset of imaging the O_2 distribution.[51,65] Besides background light, also background fluorescence of chlorophyll and other fluorescent pigments in the sample can interfere with the luminescence signal used to sense O_2. Especially in dense photosynthetic systems such as biofilms and coral tissue, this can be a significant problem and needs special sensor optimization in terms of optical isolation, tuning of the sensor composition enabling excitation outside the absorption maxima of chlorophyll, or by using a time gated readout where the fast decaying chlorophyll fluorescence is filtered out.

In conclusion, optical O_2 sensors have proved useful within extreme aquatic environments, although often special developments are needed in order to meet the challenges presented by extreme environments.

7.3.3 Sensor Stability – from Mechanical Stress to Biofouling

A key challenge for sensors in aquatic environments is mechanical and optical stability. Although often overlooked, this issue is far from solved and presents a key challenge for future sensor development and optimization. Several aspects affect the stability of optical sensors. Obviously, photostability (especially of the O_2 indicator) is a key issue. However, several O_2 indicators exhibit very good photostability and withstand extended illumination without significantly affecting the measurement.[26] The mechanical stability of optical O_2 sensors is generally high, especially when robust sensor designs are used rather than microsensors.

The major factor limiting stability and applicability of O_2 sensors in aquatic systems is biofouling. Biofouling describes the generally unwanted formation of a biological cover on any surface submerged in water. A sensor surface will first be colonized by bacterial or algal biofilms, which primes the ground for settlement of larvae and propagules of other organisms that further colonize the sensor, this includes also larger algae or even barnacles and mussels on the submerged sensor. Obviously, the formation of any sort of biological cover of the sensor (in particular the receptor) will affect the readings. Biofouling results in changed O_2 diffusion towards the sensor as well as incorrect readings due to respiration or O_2 production in the biofilm coating the sensor. Biofouling can thus strongly compromise the long term application of optical sensors for monitoring purposes in aquatic habitats.

Solutions to the biofouling problem are manifold and include mechanical as well as chemical solutions.[66] Automated wipers or brushes are commonly used for mechanical cleaning, which will prevent large organism settling on the sensor, while often not preventing the formation of thin biofilms on the sensor. Critical factors are robustness of the mechanical cleaning system as well as power consumption. Alternative mechanical systems include shutters that hide the sensor surface and only open during the measurement period. Here, copper-based shutters have proven useful, as copper also inhibits microbial growth[66] by releasing the biocide Cu^{2+}. In general, the use of biocide-releasing paints was found to be an effective anti-fouling strategy, in line with experiences from ship paints. Nevertheless, the release of a biocide might also affect the conditions around the sensor and therefore the validity of the sensor reading. Chemical modification of the sensor surface with anti-fouling or repelling layers was also investigated and showed promising results. For example a coating with a phosphorylcholine-containing polymer resulted in a sensor with reduced bio-fouling, and showed only minor effects on the sensor characteristics.[67]

Biofouling is a key limitation, when it comes to using optical O_2 sensors for long-term monitoring in aquatic habitats. Several attempts have been made to reduce biofouling, but no “golden solution” has been identified.

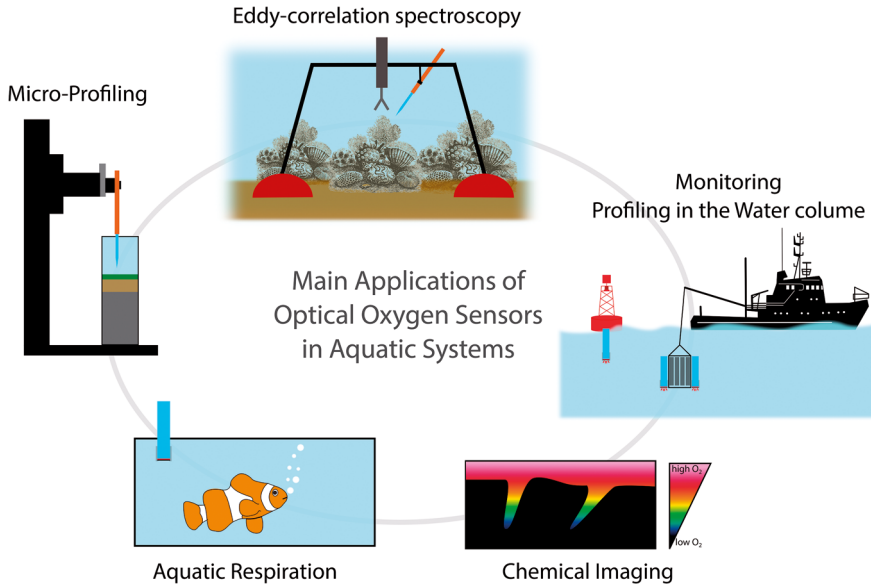

Figure 7.3 Optical O_2 sensors are applied in multiple areas of aquatic science ranging from high-resolution profiling or imaging measurements to long-term monitoring.

Most likely, such a universal solution will not be found, as the rate and species composition of biofouling on sensors is highly dependent on the environment. Nutrient availability, temperature, light exposure, flow and depth are just a few of the many environmental factors that influence biofouling. Detailed studies on both sensor materials as well as environmental factors are thus needed to get a better understanding of how to prevent biofouling and optimize long-term deployment of optical O_2 sensors in aquatic environments (Figure 7.3).

7.4 Applications of Optical O_2 Sensors

Since first introduced to aquatic science,[16] optical O_2 sensors have become widely applied in aquatic science and are now available (also commercially) in a large variety of designs and measuring characteristics. Currently, commercial optical and electrochemical O_2 sensors share the market more or less equally.

7.4.1 Application of Micro-opt(r)odes

While electrochemical microsensors have been used since the mid/end 1960s[8,11,12,68] to measure O_2 in aquatic systems, optical O_2 microsensors were first introduced to aquatic science in 1995.[16,18,35] While at first the luminescence intensity was used to quantify O_2,[16] lifetime-based measurements were introduced soon thereafter as a prerequisite for more robust sensor readout.[34] The main advantages of O_2 micro-opt(r)odes are: (i) high spatial

resolution (around 30–50 μm depending on the measuring tip diameter), (ii) fast response time (down to <1 s), and (iii) no O_2 consumption by the sensor. In contrast to O_2 microelectrodes, they are also not cross-sensitive to H_2S, which can be present in the seafloor and in biofilms. These advantages are also the main drivers of using micro-opt(r)odes. In the following some of the main areas of application will be described.

7.4.1.1 Profiling

The development and application of microsensors in aquatic science has enabled measurements of chemical concentration profiles, temperature and light profiles between the mixed water and (i) the porous seafloor sediment matrix, (ii) the exopolymer matrix of biofilms and marine snow particles, and (iii) the tissues of aquatic plants and animals.[12,14,32] Such measurements of physico-chemical gradients give detailed insight to mass transfer, radiative exposure, optical properties, and chemical transformation processes in such surface-associated aquatic systems. The introduction of O_2 microelectrodes to marine science in the mid/end 1960s[8,11,12,68] has thus lead to a detailed understanding of important mechanisms such as the diffusive boundary layer,[3] the O_2 penetration depth into sediments,[11] and the O_2 dynamics in corals.[69] The solubility of O_2 in water is much lower than in air (about 30 times) and O_2 diffuses 10 000 times slower in water as in air. At the same time, O_2 is the most energetically favorable electron acceptor for respiratory metabolism and is produced by oxygenic photosynthesis in aquatic plants, algae and cyanobacteria. This leads to the formation of O_2 concentration gradients in aquatic systems that require fine scale measurements for accurate quantification, typically at <0.1 mm spatial resolution.

Optical O_2 sensing was actually first introduced to aquatic biology by the development of O_2 microopt(r)odes.[16] Such optical microsensors have similar measuring characteristics in terms of response time and temperature dependence as electrochemical microsensors, but they are much easier to fabricate, have no intrinsic O_2 consumption and are not susceptible to *e.g.* H_2S interference. They can be used in the same types of applications as electrochemical O_2 microsensors, but also in settings where microelectrodes are challenged *e.g.* by low temperatures[62] or strong electromagnetic fields. In terms of measuring systems, very similar setups for motorized microprofiling in 1D, 2D, or even 3D configurations are commercially available for both O_2 microelectrodes and micro-opt(r)odes, which can be regarded as largely complementary techniques in most applications.

7.4.1.2 Eddy Correlation Spectroscopy

The flux of O_2 across the sediment–water interface is a good proxy for the integrated benthic carbon mineralization as well as primary production of biofilms and sediments.[1] There are several established methods to determine the O_2 uptake of sediments in the field including measurements of

O_2 concentration microprofiles[70] or by using chamber incubations of known sediment areas/volumes.[71] Both established methods use either optical or electrochemical O_2 sensors. In 2003, a new method called eddy correlation was introduced to aquatic science enabling non-invasive quantification of the net O_2 uptake/production of larger areas of sediments and other surfaces.[71] This so-called eddy-covariance or eddy-correlation method measures the covariance between two parameters simultaneously, namely the fluctuating vertical velocity component using an acoustic Doppler velocimeter and the fluctuating O_2 concentration using a microsensor within the same sampling volume. Measurements are typically performed in the turbulent boundary layer 10–50 cm above the sediment at a frequency of 14–25 Hz. As the method is non-invasive and does not need any sensor to penetrate the surface, it can be used to measure integral O_2 fluxes over large areas of complex habitats (not accessible by other means) like coral reefs,[72] hard bottom substrates,[73] seagrass meadows[74] or sea ice.[75,76]

In recent years, this technique has seen a significant boost and commercial systems are now on the market further stimulating the use of eddy correlation systems in aquatic systems. Many of these systems employ fast-responding electrochemical O_2 microsensors. As such sensors consume O_2 as part of the measurement process (contrary to optical sensors), O_2 microelectrodes have an inherent, albeit small, stirring sensitivity. It was shown that this stirring sensitivity, even if very low, can result in an artificial flux.[77] Optical O_2 microsensors were also tested in the same study and did not exhibit such artefacts. Consequently, due to the lack of stirring sensitivity and the fast response time of optical O_2 microsensors, they are now recommended as the preferred O_2 microsensor for eddy covariance measuring systems.[77] Recently a dual sensor measuring O_2 as well as temperature at the same time was developed and successfully applied for eddy covariance measurements.[78] In terms of sensor design, this sensor is rather a bulk sensor than a microsensor. Nevertheless, the achieved response time is remarkably short (t_{90} of ~0.5 s for O_2), while the sensor at the same time is more sturdy and does not show any stirring sensitivity. In the field of eddy correlation measurements, the sensor performance is essential for the data quality and the conclusions that can be drawn from the measurements. Therefore, optical sensors have a great potential in this field and have already provided excellent data.

7.4.2 Applications of Bulk Sensors and Sensor Patches

Bulk sensors or O_2 macro-opt(r)odes are characterized by a sensor tip size of ~1 mm or more. Spatial resolution is thus low and generally the response time is longer than for O_2 micro-opt(r)odes, *i.e.*, several seconds. The main benefit of these macro sensors is their improved mechanical stability. Bulk sensors come in a variety of designs and are often made to fit a certain application. In contrast to micro-opt(r)odes, bulk sensors are often constructed using cheaper plastic fibers to guide the light between the optics and the receptor.[79] Alternatively, entire sensor modules or

heads can also be constructed,[80] where the sensor material (receptor) is directly placed on top of the optical part. Sensor patches may also be seen as bulk sensors integrated into a vessel enabling external readout through a transparent wall *via* a fiber, camera or other types of detector modules (see *e.g.* Figure 7.2).

7.4.2.1 Respirometry

The O_2 consumption or production of aquatic organisms is an important physiological and environmental parameter, and such respirometric measurements involve species (or system samples) of many different sizes ranging from microorganisms to fish. Three different experimental approaches are used for respirometry: (i) closed systems, (ii) flow-through systems, and (iii) intermittent flow systems.[81] In closed systems, the sample of interest is placed inside a closed airtight vessel and O_2 consumption in the water within the vessel is followed over time. This system is the easiest to use and the only option for small species like bacteria or algae that would be washed out in a flow-through system. Flow through-systems provide a constant in and out flow of water and measure the difference in O_2 concentration between inlet and outlet to determine the respiration rate. Due to the flow regime and constant replenishment of aerated water, this system is well suited for respirometry on larger organisms during different modes of their activity (*e.g.* during swimming).[82] Intermittent flow systems combine the two other methods by repeatedly closing and opening the system. Respiration is measured in the closed system state, where after the system is flushed with aerated water to ensure removal of waste products and to reestablish ambient O_2 levels; then the cycle can start again.[83] The advantages and potential errors of the different types of respirometry are discussed elsewhere.[84,85]

In terms of sensors, a variety of O_2 sensors designs are used in respirometry. As mentioned, optical O_2 sensors do not consume O_2 during the measurement. This becomes particularly important when very low respiration rates are measured or in measurements on very small volumes. Micro-opt(r)odes can be inserted into specially designed low volume respiration chambers and are used to measure *e.g.* respiration of invertebrates or sponges.[86] This early study[86] compared micro-opt(r)odes with other commonly used methods and concluded that opt(r)ode technology is advantageous when compared to other methods due to negligible drift, ease of use and stability. Micro-opt(r)odes are used for small volume applications and are commercially available. Alternatively, also respiration vessels with integrated sensor spots (sensor patches) can be used and read out through a transparent wall using optical fibers. A variety of bulk sensors can also be inserted into respirometers *e.g.* for *in situ* sensing of O_2 in incubation chambers.[87]

An advantage of optical sensors is that they can be used at different O_2 regimes and that their sensitivity can be tuned to fit the problem. For example, trace sensors were used to measure O_2 consumption and production at

very low O_2 levels.[56,88] Photosynthetic O_2 net production can also be determined using optical sensors within closed systems.[89] When studying photosynthetic O_2 production it is, however, important to protect the sensor with an optical isolation (especially at high light levels).

7.4.2.2 Environmental Monitoring

Oxygen monitoring in the environment typically involves long-term measurements, which are important means to better understand *e.g.* biogeochemical dynamics within the environment or to monitor water quality or processes involved in water treatment. Low power consumption makes opt(r)ode system very interesting for long term monitoring, but biofouling has to be addressed and can be a limiting factor for the actual deployment time. There are several companies on the market providing optical sensors for such O_2 monitoring. Sensors can *e.g.* be mounted on conductivity-temperature-depth (CTD) profilers used for oceanographic or lake measurements[55] or be implemented on buoys for continuous measurement.[90] Electrochemical sensors still dominate this field of application, mainly for historical reasons and because this technology is well established within the field. However, opt(r)ode based devices are now increasingly used in many monitoring applications due to their better long-term stability and mechanical robustness.

Besides water monitoring, also monitoring within wetlands or riverbeds is highly relevant. For such purposes, systems based on multiple robust fiber-based O_2 sensors have been developed for long-term deployment in the environment (Figure 7.4). For example a multi-fiber O_2 opt(r)ode consisting of 100 individual sensors was constructed enabling simultaneous readout of all 100 sensors[91] by fixing the ends of all the fibers in a matrix in front of a camera system imaging all sensors at once. The fiber measuring tips can then be placed at any position within the environment,[92] and the detector system records sensor readout autonomously. In other systems, sensor fibers were arranged (along with thermocouples) along a spear that was inserted into a wetland, which enabled combined long-term (several months) *in situ* monitoring of O_2 and temperature in peat soil at 10 position over a distance of 1 m.[79] In a similar spear concept, the fibers are not fixed at one position but can be moved within the spear that is entirely coated on one side with a planar O_2 opt(r)ode.[93,94]

7.4.3 Chemical Imaging

Contrary to fiber- or electrode-based sensors, planar opt(r)ode-based sensors can also be used to image the distribution and dynamics of O_2. Imaging is achieved by using a camera as detector unit in combination with appropriate filters and excitation sources. The great advantage of this method is that 2D information on the O_2 distribution and dynamics over larger areas can be obtained, thus alleviating the inherent limitation of microsensors

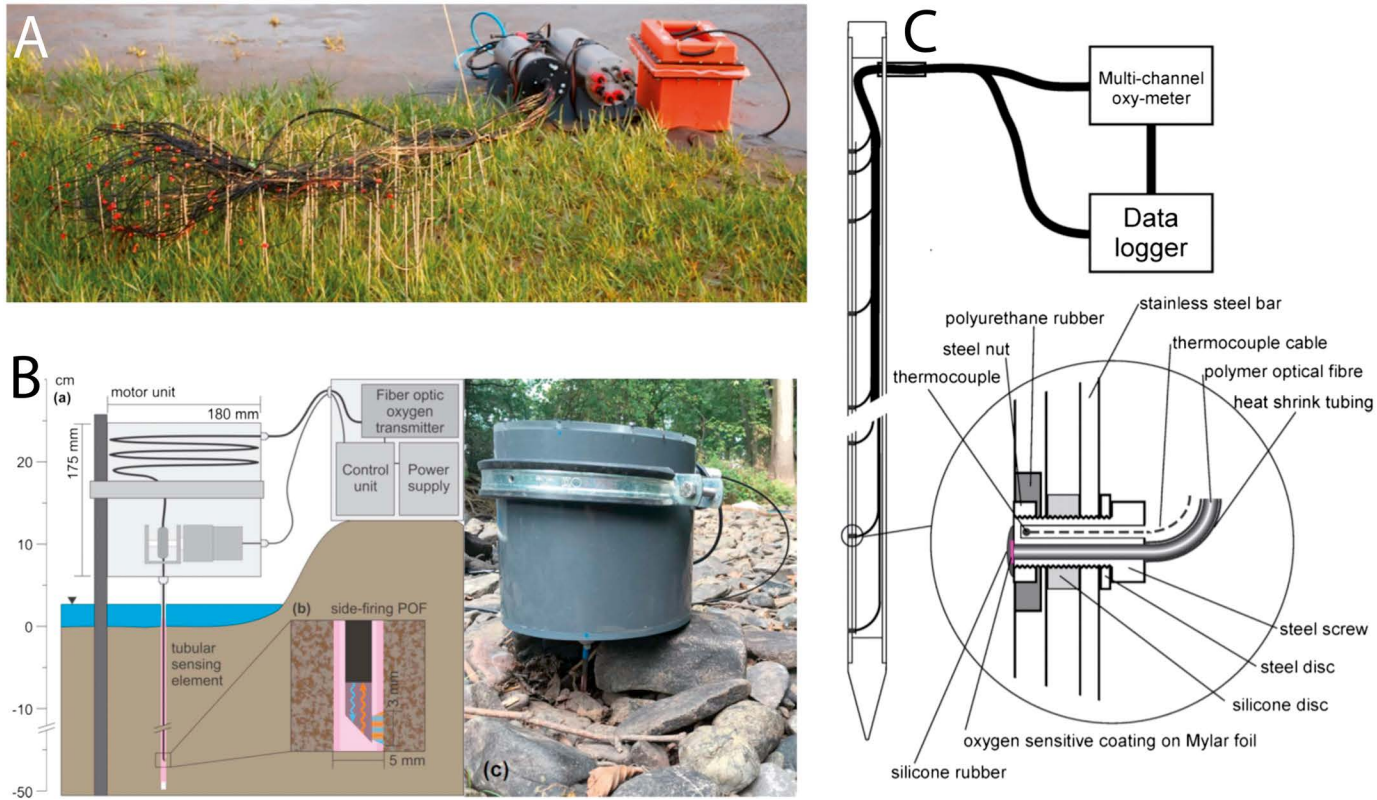

Figure 7.4 Examples of bulk optical O_2 sensors for environmental monitoring. (A) The multi-fiber O_2 opt(r)ode consisting of 100 individual sensors ready to be used in the field.[92] Reprinted from *Science of The Total Environment*, **589**, K. Koop-Jakobsen, J. Fischer and F. Wenzhöfer, Survey of sediment oxygenation in rhizospheres of the saltmarsh grass – *Spartina anglica*, 191–199,[92] Copyright © 2017 The Authors, with permission from Elsevier. (B) Visualization of the coated spear sensor that enables O_2 profiling in the environment by moving a side-firing optical fiber within the hollow spear.[93] Reprinted with permission from ref. 93. Copyright © 2017 American Chemical Society. (C) Ten O_2 sensor spots with individual fiber-optic readout and thermocouple temperature sensing elements are distributed within a 1 m long spear enabling simultaneous monitoring of O_2 and temperature.[79] Reprinted with permission from ref. 79. Copyright © 2013, the American Society of Agronomy, Crop Science Society of America, and Soil Science Society of America, Inc.

to a few point measurements. This enables visualization of the spatio-temporal heterogeneity in O_2 concentration at different scales. Depending on the chosen setup, O_2 images with high spatial resolution (<50 μm) can be obtained or larger areas (up to entire root systems) can be imaged simultaneously.[95] The possibility to visualize heterogeneities and dynamics at once as well as the possibility of combining O_2 imaging with structural or other imaging techniques (*e.g.* chlorophyll fluorescence) makes this technique highly interesting for different applications in aquatic systems.[45,96] Such measurements have mainly employed planar-opt(r)odes but recently also particle based methods have been applied.[19,20,51] While such chemical imaging was initially purely intensity-based, more robust referenced measurements now use either lifetime-based[40,97] or ratiometric[41] imaging systems. Such O_2 imaging has now been implemented in a variety of applications ranging from microscopic imaging (Figure 7.5(1)) of O_2 dynamics in biofilms,[33,98] organisms[51,99] and in sediments,[28,41] including the development of special imaging systems for *in situ* O_2 imaging[39] (Figure 7.5(2)). In the following, we present just a few of these applications representative of O_2 imaging at different spatial scales.

7.4.3.1 Microscopic O_2 Imaging

By mounting a lifetime-based or ratiometric luminescence imaging system on a microscope[22,33,98,100] or *e.g.* by using a simple USB-based microscope equipped with excitation LED's and a long-pass filter,[101–103] the O_2 distribution and dynamics can be imaged at very high (μm) spatial resolution at the level of a few cell clusters or biofilms. For microscopic imaging with planar sensors, it is important to apply very thin planar opt(r)odes to avoid the receptor layer acting as an O_2 reservoir and/or O_2 diffusion matrix, which would lead to smearing effects and low spatio-temporal resolution. Thin sub-μm receptor layers can *e.g.* be immobilized *via* spin-coating onto glass cover slips, which are silanized to facilitate better binding between the glass and receptor layer.[33] Such coverslip sensors can be constructed to exhibit near-ideal Stern–Volmer quenching by O_2, and they have a well-defined temperature response. By mounting coverslip sensors as lids in flow-chambers or membrane filtration reactors (Figure 7.5), it is possible to monitor the O_2 concentration gradients and dynamics relative to the distribution of the cellular biomass in biofilms using simple ratiometric imaging approaches.[98,100] Higher resolution studies combining O_2 imaging with laser confocal scanning microscopy on aquatic biofilms have also been realized.[33]

While the above mentioned examples of application mainly have involved cell/biofilm growth on planar opt(r)odes, microscopic O_2 imaging can also employ sensor micro- or nano-particles,[104–106] albeit few applications have so far been realized in aquatic science, where most particle-based imaging has been done at a more macroscopic level.[19,20,51,107]

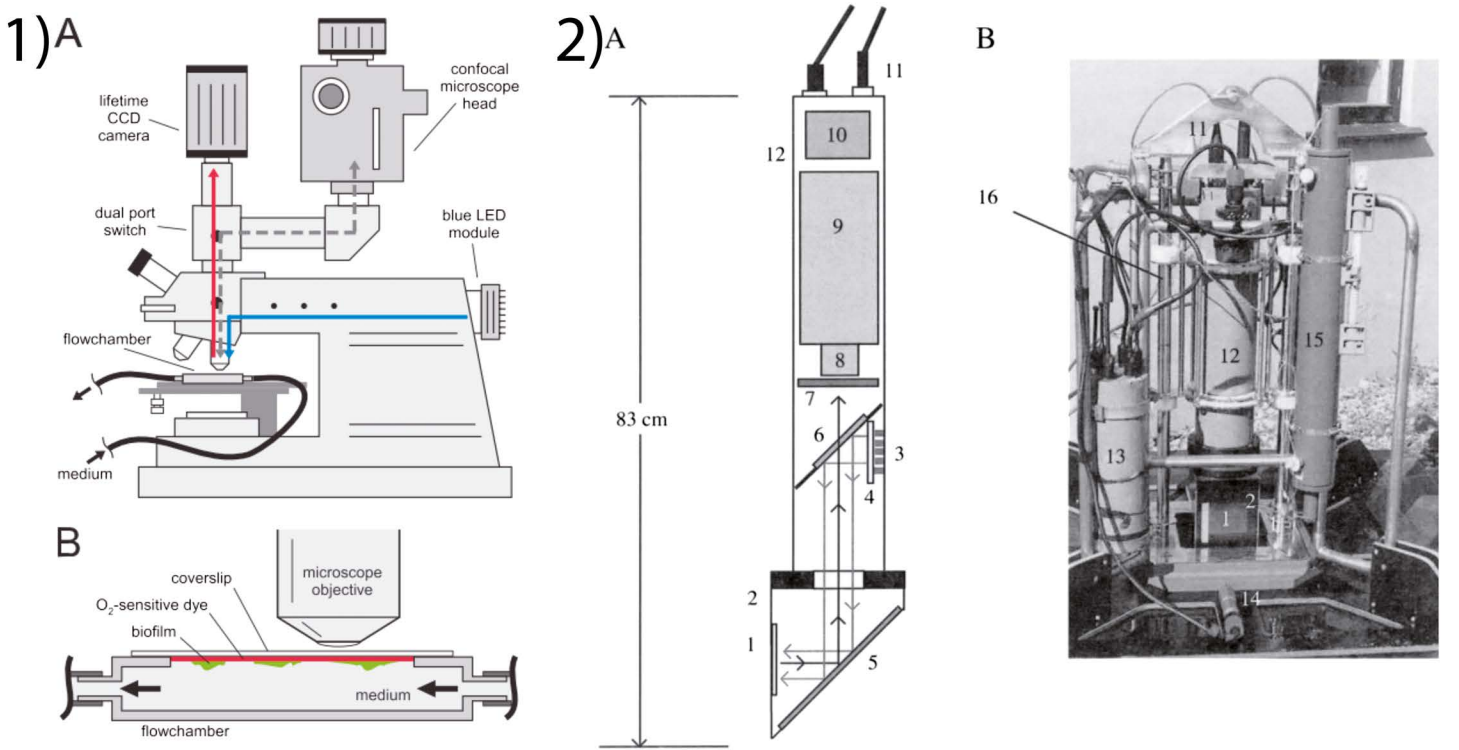

Figure 7.5 (1) Setup for microscopic O_2 imaging[33] consisting of a luminescence lifetime-based camera system mounted on a confocal microscope (A) and a flow chamber with an integrated O_2 opt(r)ode. (2) *In situ* O_2 imaging system[39] consisting of multiple components: (1) Planar opt(r)ode, (2) sensor window, (3) LEDs, (4) diffuser, (5) mirror, (6) dichroic mirror, (7) excitation filter, (8) lens, (9) CCD camera, (10) electronics controlling the excitation light, (11) connectors, (12) central housing, (13) battery for video and light, (14) video camera, (15) Niskin bottle, and (16) positioning elevator (further details in ref. 39). Reproduced with permission from ref. 39, © 2001, by the Association for the Sciences of Limnology and Oceanography, Inc. and ref. 33, Copyright 2007, American Society for Microbiology.

7.4.3.2 O_2 Imaging in Sediments

Knowledge about the O_2 distribution and dynamics in sediments is crucial for the understanding of overall carbon mineralization and the zonation of different aerobic and anaerobic processes involved in overall carbon and nutrient cycling. Dependent on the composition of the sediment and its associated fauna and flora, a distinct mosaic of oxic and anoxic micro-niches can establish within the sediment.[108] When first introduced, planar opt(r)odes already showed heterogeneities in the diffusive boundary layer due to the topography of the sediment and also hotspots of O_2 consumption due to variations in available labile carbon.[28] In the presence of macrofauna such as burrowing animals, the O_2 availability within the sediment can exhibit extreme spatio-temporal heterogeneity.[64] Planar opt(r)odes are ideal tools to visualize such effects of burrowing animals on the O_2 availability within sediments.[108] By confining burrowing animals close to the planar opt(r)ode, it is *e.g.* possible to study the sediment O_2 dynamics associated with the bio-irrigation of the burrow and consequently the changes in the surrounding sediment layers (Figure 7.6).[41,109] Such studies can be done at various scales depending on the sediment characteristics and animal sizes, as planar opt(r)odes and the measuring systems can easily by adapted for measurements even over several 10th of cm^2. Besides lab-based studies, such effects of bio-irrigation and bioturbation can also be observed *in situ* using special autonomous instruments platforms for planar opt(r)ode-based chemical imaging.[39,110]

Recently, also sensor particles were used to study the dynamics of bioturbation at the water sediment interface (Figure 7.6). For this purpose a special lifetime-based method was developed that uses a laser sheet to excite O_2 sensor nanoparticles dispersed within the overlaying water.[107] This enabled the imaging of the outburst of anoxic water from a ventilating burrow, which could be followed without disturbing the natural flow.

Besides the effects of fauna, aquatic plants can also strongly impact the O_2 dynamics within sediments. As an example, seagrasses transport O_2 from the leaves to their roots, where O_2 is released at their root tips[111] protecting the most sensitive parts of below-ground plant tissue against intrusion of toxic H_2S from the surrounding sediment. Chemical imaging enables visualization of such hotspots and can be used to study dynamic O_2 changes in the plant rhizosphere *e.g.* as a function of light exposure of the leaves or the O_2 content of the surrounding water (Figure 7.7).[43] Similar O_2 transport towards the roots is found in other aquatic[110] or water locked plants like rice.[112] For example, a recent study monitored the effect of O_2 release from the roots of the salt marsh grass *Spartina anglica* on the bulk sediment. By using both planar-opt(r)odes and bulk sensors, the authors could show that the effect is very localized and is not sufficient to significantly aerate the bulk sediment.[97]

Planar opt(r)odes were first applied to map the O_2 dynamics in the seagrass rhizosphere,[43,113] while sensor nanoparticles were applied more recently enabling similar resolution but larger coverage of the complete rhizosphere. For particle-based O_2 imaging, seagrass specimens were grown in an artificial

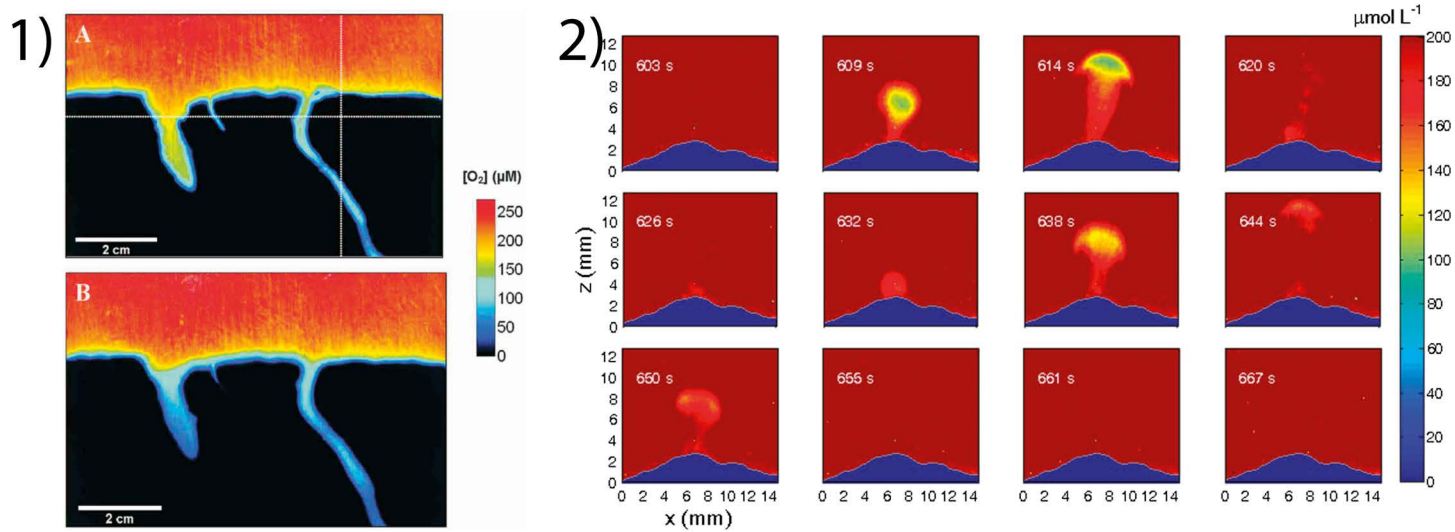

Figure 7.6 Examples of O_2 imaging in and above aquatic sediments. (1) O_2 imaging using ratiometric readout of a planar opt(r)ode inserted in a sediment with burrowing animals.[41] (2) Ejection of anoxic water from a worm burrow visualized with sensor nanoparticles in the water above the water–sediment interface.[107] Reproduced with permission from ref. 41, © 2011, by the Association for the Sciences of Limnology and Oceanography, Inc. and ref. 107, © 2016 Association for the Sciences of Limnology and Oceanography.

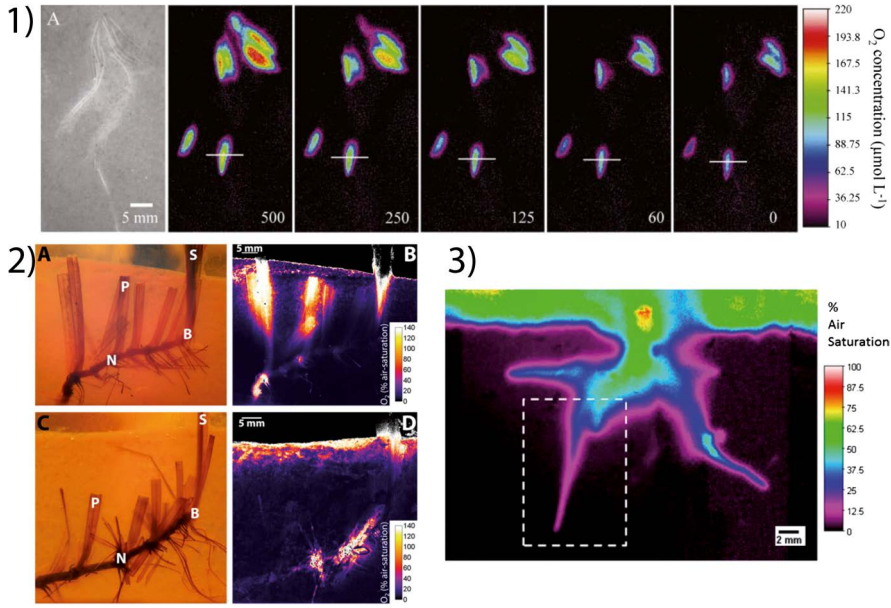

Figure 7.7 Examples of planar opt(r)ode- and nanoparticle-based imaging of O_2 in the rhizosphere of aquatic plants. Oxygenation around the roots of aquatic plants can be visualized by using planar opt(r)odes like shown in (1)[43] and (3)[112] or by embedding the plant in a sensor nanoparticle containing agar (2).[20] Reproduced with permission from ref. 43, © 2006, by the Association for the Sciences of Limnology and Oceanography, Inc.; ref. 20. Copyright 2015 American Chemical Society, and P. N. Williams, *et al.*, *Environ. Sci. Technol.*, 2014, **48**, 8498–8506,[112] under a CC BY 4.0 license, https://creativecommons.org/licenses/by/4.0/. Copyright © 2014 American Chemical Society.

agar-based sediment resembling the natural sediment in terms of H_2S content and pH. Addition of O_2 sensor nanoparticles to the artificial sediment matrix enabled visualization of O_2 microenvironments over the entire root system.[19,20] Such measurements were used to study the effects of rising water temperature and hypoxia on the O_2 transport to the rhizosphere.

In summary, planar opt(r)ode-based as well as more recently developed particle-based O_2 imaging has yielded numerous novel insights to factors regulating the O_2 microenvironment in sediments and rhizospheres.[108]

7.4.3.3 O_2 Imaging on Structurally Complex Samples

Soft samples like sediments are easy to manipulate, and it is relatively easy to bring the opt(r)ode into contact with the sample or to insert microsensors for profiling, while measurements on hard and/or structurally complex samples are more challenging. For such systems, both planar opt(r)ode- and particle-based O_2 imaging has great advantages (see examples in Figure 7.8).

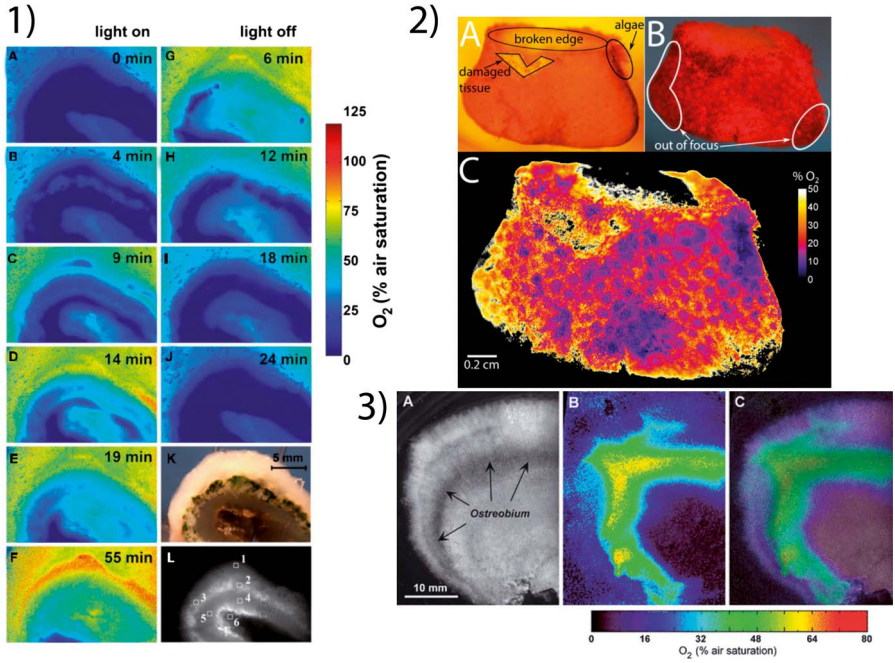

Figure 7.8 Examples of planar opt(r)ode- and particle-based O_2 imaging of structurally challenging samples: (1) light dependent O_2 dynamics of a ascidian sample visualized by pressing it against a planar opt(r)ode.[99] Reprinted from Kühl *et al.*, *Front. Microbiol.*, 2012, **3**, 402,[99] https://doi.org/10.3389/fmicb.2012.00402. © 2012 Kühl, Behrendt, Trampe, Qvortrup, Schreiber, Borisov, Klimant and Larkum. Published under the CC BY 3.0 licence, https://creativecommons.org/licenses/by/3.0/. (2) Surface O_2 imaging of a coral fragment enabled by spray-painting the sample with sensor nanoparticles.[51] Reprinted from *Sensors and Actuators B: Chemical*, **237**, K. Koren, S. L. Jakobsen and M. Kühl, *In vivo* imaging of O_2 dynamics on coral surfaces spray-painted with sensor nanoparticles, 1095–1101,[51] Copyright 2016, with permission from Elsevier; (3) O_2 dynamics in the endolithic subsurface algal communities of a stony coral visualized by pressing the sample against a planar opt(r)ode.[21] Reproduced from ref. 21 with permission from John Wiley and Sons Inc. © 2008 Phycological Society of America.

Imaging of the O_2 dynamics in endolithic subsurface algal communities of stony corals have *e.g.* been done with planar opt(r)odes.[21] For this, a smooth vertical cross-section through the hard coral skeleton was put in contact with a planar-opt(r)ode.[21] Another structurally complex sample is the symbiont-containing ascidian *Lissoclinum patella*, which forms a cartilage-like structure with internal populations of microbial symbionts.[99] Cross-sections through the ascidians were pressed against a planar opt(r)ode[99] enabling mapping of strong O_2 dynamics due to photosynthesis and respiration at a scale of several cm^2.

While cutting is a possible way to enable O_2 imaging for certain samples, it is certainly not a universal solution. A way to study the O_2 dynamics on complex surfaces is to coat the surface with sensor material. Potentially a planar opt(r)ode could be pressed onto the surface, but in this case the sensor foil will act as a diffusion barrier imposing strong artefacts. The application of optical O_2 sensor particles can overcome or minimize this problem. It was demonstrated that micro-[22] as well as nanoparticle[51] based O_2 sensors can be used to visualize the dynamics on the surface of corals. The magnetic microparticles were held in place on the coral with the help of a strong magnet placed underneath the coral. For the nanoparticles a spray-painting approach was chosen, which yielded homogeneous coverage of the studied species without any detectable short-term harm of the investigated coral. Such distributed sensing with O_2 sensor particles has just been introduced to aquatic science and holds a strong potential for novel applications in natural samples with complex surface topography.

7.5 Future Challenges

Optical O_2 sensors are the most advanced optical sensors on the market. Many applications have been made possible by this technology especially in aquatic environments. So the question arises – what is coming next for optical O_2 sensors?

7.5.1 Multi-analyte Measurements

There is now an increasing interest in further combining and developing optical sensors for multi-analyte sensing and imaging. As O_2 sensors are so well developed and many different indicators are available, they are ideal for muli-analyte chemical imaging systems. Dual optical sensors for imaging O_2 and pH;[65] O_2 and CO_2,[114] and O_2 and temperature[29] have already been described and partly tested on aquatic samples.[65] Besides combining two optical sensors within a planar setup, the combination of O_2 sensors with other analytical techniques is of interest. For example, diffusive gradients in thin films (DGT) is an exciting technology enabling 2D ion sensing. Similar to planar-opt(r)odes, this method also uses thin films and can be put on top of an opt(r)ode[45,115] and such combined sensing bears a strong potential in various aquatic systems.[116]

Multiplexing of different sensor materials for multi-analyte measurements is also of interest for the development of novel fiber-based sensors. This can be facilitated either by combining several fibers or sensing positions for different analytes[117,118] or by combining several sensing functionalities within one fiber.[119] Either way, cross-sensitivities need to be minimized and easy calibration protocols need to be established in order to allow multi-analyte sensing to find its way into real world applications. Once the usability is there, the possible applications are endless.

7.5.2 Special O_2 Microniches and Their Impact on Other Process

Several processes in aquatic systems are dependent on certain O_2 concentrations. For example, dinitrogen (N_2) fixation and denitrification are favored at hypoxic or anoxic conditions. Dinitrogen fixing filamentous cyanobacteria localize this process in specialized cell, the so-called heterocysts, that exhibit hypoxia or anoxia. Also within marine snow, low O_2 concentrations are expected to favor N_2 fixation and other anaerobic processes. However, only few microsensor based studies have investigated the O_2 microenvironment in these systems. Nanoparticle-based O_2 sensors or dissolved O_2 indicators that find use in cell culture experiments,[104,120–122] could be used to stain such cyanobacteria or marine snow particles enabling mapping of O_2 concentrations using *e.g.* lifetime-based O_2 microscopy. First experiments in this direction were made when looking into the O_2 levels within copepod carcasses.[123] These measurements showed that the inside of carcasses can easily be anoxic, even in fully air saturated waters. Knowledge of such anoxic microniches in aerated aquatic habitats is still scarce, but the application of high-resolution optical O_2 sensing and imaging methodology for studying O_2 microenvironments seems very promising.

7.5.3 Low Cost Instrumentation for Long-term Monitoring

A better understanding of the O_2 dynamics at larger spatial and temporal scales is still needed in many, if not all, aquatic systems. This calls for relatively low cost robust O_2 sensors that can be widely deployed for long-term environmental monitoring, and here optical O_2 sensor technology is the way to go as such sensor systems consume less energy and can be produced relatively cheaply as compared to electrochemical sensors. This is a rapidly developing field, which will supplement existing monitoring sensor networks. As mentioned, a major challenge for such monitoring is sensor stability and in particular biofouling.

7.6 Conclusions

Since its introduction to aquatic science in 1995,[16] the technology for optical O_2 sensing in aquatic systems has undergone astonishing development now encompassing fiber-optic micro- and macro-sensors, sensor patches for remote readout, planar opt(r)odes, as well as nano- and micro-particle based sensors for mapping O_2 concentration and dynamics at high spatial resolution. Furthermore, optical sensors for multi-parameter chemical sensing are now also available for application in aquatic science. While this development has largely been driven by interdisciplinary efforts of analytical chemists, biologist and engineers, the market for optical O_2 sensors has also increased enormously. A large diversity of optical O_2 sensors is commercially available, and optical O_2 sensing is now considered a standard technique in many areas of aquatic science.

References

1. R. N. Glud, *Mar. Biol. Res.*, 2008, **4**, 243–289.
2. T. R. Marrero and E. A. Mason, *J. Phys. Chem. Ref. Data*, 1972, **1**, 3–118.
3. B. B. Jørgensen and N. P. Revsbech, *Limnol. Oceanogr.*, 1985, **30**, 111–122.
4. *The Benthic Boundary Layer: Transport Processes and Biogeochemistry: Transport Processes and Biogeochemistry*, ed. B. P. Boudreau and B. B. Jørgensen, Oxford University Press, New York, USA, 2001.
5. L. W. Winkler, *Ber. Dtsch. Chem. Ges.*, 1888, **21**, 2843–2854.
6. L. C. Clark, R. Wolf, D. Granger and Z. Taylor, *J. Appl. Physiol.*, 1953, **6**, 189–193.
7. E. Gnaiger and H. Forstner, *Polarographic Oxygen Sensors: Aquatic and Physiological Applications*, Springer, Berlin Heidelberg, 1983.
8. N. P. Revsbech, *Limnol. Oceanogr.*, 1989, **34**, 474–478.
9. N. P. Revsbech, L. H. Larsen, J. Gundersen, T. Dalsgaard, O. Ulloa and B. Thamdrup, *Limnol. Oceanogr.: Methods*, 2009, **7**, 371–381.
10. N. P. Revsbech, J. Sorensen, T. H. Blackburn and J. P. Lomholt, *Limnol. Oceanogr.*, 1980, **25**, 403–411.
11. N. P. Revsbech, B. B. Jørgensen and T. H. Blackburn, *Science*, 1980, **207**, 1355–1356.
12. N. P. N. Revsbech and B. B. B. Jørgensen, *Adv. Microb. Ecol.*, 1986, **9**, 293–352.
13. M. Fazli, T. Bjarnsholt, K. Kirketerp-Møller, A. Jørgensen, C. B. Andersen, M. Givskov and T. Tolker-Nielsen, *Wound Repair Regen.*, **19**, 387–391.
14. M. Kühl and N. P. Revsbech, in *The Benthic Boundary Layer: Transport Processes and Biogeochemistry*, ed. B. B. Boudreau and B.P. Jørgensen, Oxford University Press, New York, 2001, pp. 180–210.
15. H. Kautsky and A. Hirsch, *Ber. Dtsch. Chem. Ges. (A B Ser.)*, 1931, **64**, 2677–2683.
16. I. Klimant, V. Meyer and M. Kuhl, *Limnol. Oceanogr.*, 1995, **40**, 1159–1165.
17. R. McFarlane and M. C. Hamilton, *International Society for Optics and Photonics*, ed. A. M. Verga Scheggi, 1987, pp. 324–330.
18. I. Klimant, G. Hoist and M. Kühi, *Proc. SPIE-Int. Soc. Opt. Eng.*, 1995, **2508**, 375–386.
19. K. E. Brodersen, K. Koren, M. Lichtenberg and M. Kühl, *Plant, Cell Environ.*, 2016, 1619–1630.
20. K. Koren, K. E. Brodersen, S. L. Jakobsen and M. Kühl, *Environ. Sci. Technol.*, 2015, **49**, 2286–2292.
21. M. Kühl, G. Holst, A. W. D. Larkum and P. J. Ralph, *J. Phycol.*, 2008, **44**, 541–550.
22. J. Fabricius-Dyg, G. Mistlberger, M. Staal, S. M. Borisov, I. Klimant and M. Kühl, *Mar. Biol.*, 2012, **159**, 1621–1631.
23. J. N. Demas, B. A. DeGraff and W. Xu, *Anal. Chem.*, 1995, **67**, 1377–1380.
24. E. R. Carraway, J. N. Demas, B. A. DeGraff and J. R. Bacon, *Anal. Chem.*, 1991, **63**, 337–342.
25. X.-D. Wang and O. S. Wolfbeis, *Chem. Soc. Rev.*, 2014, **43**, 3666–3761.
26. M. Quaranta, S. M. Borisov and I. Klimant, *Bioanal. Rev.*, 2012, **4**, 115–157.

27. K. Koren, L. Hutter, B. Enko, A. Pein, S. M. Borisov and I. Klimant, *Sens. Actuators, B*, 2013, **176**, 344–350.
28. R. Glud, N. Ramsing, J. K. Gundersen and I. Klimant, *Mar. Ecol.: Prog. Ser.*, 1996, **140**, 217–226.
29. S. M. Borisov, A. S. Vasylevska, C. Krause and O. S. Wolfbeis, *Adv. Funct. Mater.*, 2006, **16**, 1536–1542.
30. L. F. Rickelt, L. D. M. Ottosen and M. Kühl, *Sens. Actuators, B*, 2015, **211**, 462–468.
31. G. Holst, I. Klimant, O. Kohls and M. Kühl, *Chemical Sensors in Oceanography*, 2000, pp. 143–188.
32. M. Kühl, *Methods Enzymol.*, 2005, **397**, 166–199.
33. M. Kühl, L. F. Rickelt and R. Thar, *Appl. Environ. Microbiol.*, 2007, **73**, 6289–6295.
34. I. Klimant, M. Kühl, R. N. Glud and G. Holst, *Sens. Actuators, B*, 1997, **38**, 29–37.
35. G. Holst, M. Kühl and I. Klimant, *Proc. SPIE*, 1995, **2508**, 387–398.
36. G. Holst, O. Kohls, I. Klimant, B. König, M. Kühl and T. Richter, *Sens. Actuators, B*, 1998, **51**, 163–170.
37. S. Schreml, R. J. Meier, M. Kirschbaum, S. C. Kong, S. Gehmert, O. Felthaus, S. Küchler, J. R. Sharpe, K. Wöltje, K. T. Weiß, M. Albert, U. Seidl, J. Schröder, C. Morsczeck, L. Prantl, C. Duschl, S. F. Pedersen, M. Gosau, M. Berneburg, O. S. Wolfbeis, M. Landthaler and P. Babilas, *Theranostics*, 2014, **4**, 721–735.
38. J. P. Fischer and F. Wenzhöfer, *Limnol. Oceanogr.: Methods*, DOI: 10.4319/lom.2010.8.254.
39. R. N. Glud, A. Tengberg, M. Kühl, P. O. J. Hall and I. Klimant, *Limnol. Oceanogr.*, 2001, **46**, 2073–2080.
40. G. Holst and B. Grunwald, *Sens. Actuators, B*, 2001, **74**, 78–90.
41. M. Larsen, S. M. Borisov, B. Grunwald, I. Klimant and R. N. Glud, *Limnol. Oceanogr.: Methods*, 2011, **9**, 348–360.
42. R. J. Meier, L. H. Fischer, O. S. Wolfbeis and M. Schäferling, *Sens. Actuators, B*, 2013, **177**, 500–506.
43. M. S. Frederiksen and R. N. Glud, *Limnol. Oceanogr.*, 2006, **51**, 1072–1083.
44. R. N. Glud, F. Wenzhöfer, A. Tengberg, M. Middelboe, K. Oguri and H. Kitazato, *Deep Sea Res., Part I*, 2005, **52**, 1974–1987.
45. J. Santner, M. Larsen, A. Kreuzeder and R. N. Glud, *Anal. Chim. Acta*, 2015, **878**, 9–42.
46. P. Lehner, C. Larndorfer, E. Garcia-Robledo, M. Larsen, S. M. Borisov, N.-P. Revsbech, R. N. Glud, D. E. Canfield and I. Klimant, *PLoS One*, 2015, **10**, e0128125.
47. G. Mistlberger, K. Koren, E. Scheucher, D. Aigner, S. M. Borisov, A. Zankel, P. Pölt and I. Klimant, *Adv. Funct. Mater.*, 2010, **20**, 1842–1851.
48. S. M. Borisov, T. Mayr, G. Mistlberger, K. Waich, K. Koren, P. Chojnacki and I. Klimant, *Talanta*, 2009, **79**, 1322–1330.
49. K. Koren, G. Mistlberger, D. Aigner, S. M. Borisov, A. Zankel, P. Pölt and I. Klimant, *Monatsh. Chem.*, 2010, **141**, 691–697.

50. S. M. Borisov, A. Torsten Mayr and I. Klimant, DOI: 10.1021/AC071374E.
51. K. Koren, S. L. Jakobsen and M. Kühl, *Sens. Actuators, B*, 2016, 19–21.
52. A. Paulmier and D. Ruiz-Pino, *Prog. Oceanogr.*, DOI: 10.1016/j.pocean.2008.08.001.
53. D. E. Canfield, F. J. Stewart, B. Thamdrup, L. De Brabandere, T. Dalsgaard, E. F. Delong, N. P. Revsbech and O. Ulloa, *Science*, DOI: 10.1126/science.1196889.
54. J. J. Childress and B. A. Seibel, *J. Exp. Biol*.
55. M. Larsen, P. Lehner, S. M. Borisov, I. Klimant, J. P. Fischer, F. J. Stewart, D. E. Canfield and R. N. Glud, *Limnol. Oceanogr.: Methods*, 2016, **14**, 784–800.
56. E. Garcia-Robledo, C. C. Padilla, M. Aldunate, F. J. Stewart, O. Ulloa, A. Paulmier, G. Gregori and N. P. Revsbech, *Proc. Natl. Acad. Sci. U. S. A.*, 2017, **114**, 8319–8324.
57. P. Lehner, C. Staudinger, S. M. Borisov and I. Klimant, *Nat. Commun.*, 2014, **5**, 4460.
58. N. P. Revsbech, B. Thamdrup, T. Dalsgaard and D. E. Canfield, *Methods Enzymol.*, 2010, **486**, 325–341.
59. R. N. Glud, I. Klimant, G. Holst, O. Kohls, V. Meyer, M. Kühl and J. K. Gundersen, *Deep Sea Res., Part I*, 1999, **46**, 171–183.
60. T. Fenchel and B. Finlay, *Biol. Rev. Cambridge Philos. Soc.*, 2008, **83**, 553–569.
61. K. Hancke, B. K. Sorrell, L. Chresten Lund-Hansen, M. Larsen, T. Hancke and R. N. Glud, *Limnol. Oceanogr.*, 2014, **59**, 1599–1611.
62. T. Mock, G. S. Dieckmann, C. Haas, A. Krell, J.-L. Tison, A. L. Belem, S. Papadimitriou and D. N. Thomas, *Aquat. Microb. Ecol.*, 2002, **29**, 297–306.
63. T. Mock, M. Kruse and G. S. Dieckmann, *Aquat. Microb. Ecol.*, 2003, **30**, 197–205.
64. H. Satoh and S. Okabe, *Microbes Environ.*, 2013, **28**, 166–179.
65. M. Moßhammer, M. Strobl, M. Kühl, I. Klimant, S. M. Borisov and K. Koren, *ACS Sens.*, 2016, **1**, 681–687.
66. L. Delauney, C. Compare and M. Lehaitre, *Ocean Sci.*, 2010, **6**, 503–511.
67. F. Navarro-Villoslada, G. Orellana, M. C. Moreno-Bondi, T. Vick, M. Driver, G. Hildebrand and K. Liefeith, *Anal. Chem.*, 2001, **73**, 5150–5156.
68. H. R. Bungay, W. J. Whalen and W. M. Sanders, *Biotechnol. Bioeng.*, 1969, **11**, 765–772.
69. M. Kühl, Y. Cohen, T. Dalsgaard, B. B. Jørgensen and N. P. Revsbech, *Mar. Ecol.: Prog. Ser.*, 1995, **117**, 159–172.
70. C. E. Reimers, K. M. Fischer, R. Merewether, K. L. Smith and R. A. Jahnke, *Nature*, 1986, **320**, 741–744.
71. R. Nøhr Glud, J. K. Gundersen, N. P. Revsbech, B. B. Jorgensen and M. Hüttel, *Deep Sea Res., Part I*, 1995, **42**, 1029–1042.
72. M. H. Long, P. Berg, D. de Beer and J. C. Zieman, *PLoS One*, 2013, **8**, e58581.

73. R. Glud, P. Berg, A. Hume, P. Batty, M. Blicher, K. Lennert and S. Rysgaard, *Mar. Ecol.: Prog. Ser.*, 2010, **417**, 1–12.
74. A. C. Hume, P. Berg and K. J. McGlathery, *Limnol. Oceanogr.*, 2011, **56**, 86–96.
75. M. H. Long, D. Koopmans, P. Berg, S. Rysgaard, R. N. Glud and D. H. Søgaard, *Biogeosciences*, 2012, **9**, 1957–1967.
76. B. G. T. Else, S. Rysgaard, K. Attard, K. Campbell, O. Crabeck, R. J. Galley, N. X. Geilfus, M. Lemes, R. Lueck, T. Papakyriakou and F. Wang, *Cold Reg. Sci. Technol.*, 2015, **119**, 158–169.
77. M. Holtappels, C. Noss, K. Hancke, C. Cathalot, D. F. McGinnis, A. Lorke and R. N. Glud, *PLoS One*, 2015, **10**, e0116564.
78. P. Berg, D. J. Koopmans, M. Huettel, H. Li, K. Mori and A. Wüest, *Limnol. Oceanogr.: Methods*, 2016, **14**, 151–167.
79. L. F. F. Rickelt, L. Askaer, E. Walpersdorf, B. Elberling, R. N. N. Glud and M. Kühl, *J. Environ. Qual.*, 2013, **42**, 1267.
80. A. Tengberg, J. Hovdenes, H. J. Andersson, O. Brocandel, R. Diaz, D. Hebert, T. Arnerich, C. Huber, A. Körtzinger, A. Khripounoff, F. Rey, C. Rönning, J. Schimanski, S. Sommer and A. Stangelmayer, *Limnol. Oceanogr.: Methods*, 2006, **4**, 7–17.
81. M. B. S. Svendsen, P. G. Bushnell and J. F. Steffensen, *J. Fish Biol.*, 2016, **88**, 26–50.
82. S. Gerile and J. Pirhonen, *Aquaculture*, 2017, **479**, 616–618.
83. J. W. Behrens, M. Van Deurs and E. A. F. Christensen, *PLoS One*, 2017, **12**, e0176038.
84. J. F. Steffensen, *Fish Physiol. Biochem.*, 1989, **6**, 49–59.
85. D. Chabot, J. F. Steffensen and A. P. Farrell, *J. Fish Biol.*, 2016, **88**, 81–121.
86. S. Gatti, T. Brey, W. Müller, O. Heilmayer and G. Holst, *Mar. Biol.*, 2002, **140**, 1075–1085.
87. J. Woelfel, K. Sørensen, M. Warkentin, S. Forster, A. Oren and R. Schumann, *Aquatic Microbial Ecology*, 2009, vol. 56, pp. 263–273.
88. X. Gong, E. Garcia-Robledo, A. Schramm and N. P. Revsbech, *Appl. Environ. Microbiol.*, 2015, **82**, 1412–1422.
89. E. Trampe, P. J. Hansen and M. Kuhl, *Algae*, 2015, **30**, 103–119.
90. M. Martini, B. Butman and M. J. Mickelson, *J. Atmos. Ocean Tech.*, 2007, **24**, 1924–1935.
91. J. P. Fischer and K. Koop-Jakobsen, *Sens. Actuators, B*, 2012, **168**, 354–359.
92. K. Koop-Jakobsen, J. Fischer and F. Wenzhöfer, *Sci. Total Environ.*, 2017, **589**, 191–199.
93. T. Brandt, M. Vieweg, G. Laube, R. Schima, T. Goblirsch, J. H. Fleckenstein and C. Schmidt, *Environ. Sci. Technol.*, 2017, **51**, 9970–9978.
94. M. Vieweg, N. Trauth, J. H. Fleckenstein and C. Schmidt, *Environ. Sci. Technol.*, 2013, **47**, 9858–9865.
95. N. Rudolph-Mohr, P. Vontobel and S. E. Oswald, *Ann. Bot.*, 2014, **114**, 1779–1787.
96. M. Kühl and L. Polerecky, *Aquat. Microb. Ecol.*, 2008, **53**, 99–118.
97. K. Oguri, H. Kitazato and R. N. Glud, *Mar. Chem.*, 2006, **100**, 95–107.

98. M. Staal, S. M. M. Borisov, L. F. F. Rickelt, I. Klimant and M. Kühl, *J. Microbiol. Methods*, 2011, **85**, 67–74.
99. M. Kühl, L. Behrendt, E. Trampe, K. Qvortrup, U. Schreiber, S. M. Borisov, I. Klimant and A. W. D. Larkum, *Front Microbiol.*, 2012, **3**, 402.
100. E. I. Prest, M. Staal, M. Kühl, M. C. M. van Loosdrecht and J. S. Vrouwenvelder, *J. Membr. Sci.*, 2012, **392–393**, 66–75.
101. F. Zhu, D. Baker, J. Skommer, M. Sewell and D. Wlodkowic, *Cytometry, Part A*, 2015, **87**, 446–450.
102. H. Tschiersch, G. Liebsch and A. Stangelmayer, *Microsensors*, InTech, 2011, pp. 281–285.
103. K. E. Brodersen, D. A. Nielsen, P. J. Ralph and M. Kühl, *Mar. Biol.*, DOI: 10.1007/s00227-014-2542-3.
104. A. V. Kondrashina, R. I. Dmitriev, S. M. Borisov, I. Klimant, I. O'Brien, Y. M. Nolan, A. V. Zhdanov and D. B. Papkovsky, *Adv. Funct. Mater.*, 2012, **22**, 4931–4939.
105. A. Fercher, S. M. Borisov, A. V. Zhdanov, I. Klimant and D. B. Papkovsky, *ACS Nano*, 2011, **5**, 5499–5508.
106. R. I. Dmitriev, S. M. Borisov, H. Düssmann, S. Sun, B. J. Müller, J. Prehn, V. P. Baklaushev, I. Klimant and D. B. Papkovsky, *ACS Nano*, 2015, **9**, 5275–5288.
107. E. Murniati, D. Gross, H. Herlina, K. Hancke, R. N. Glud and A. Lorke, *Limnol. Oceanogr.: Methods*, DOI: 10.1002/lom3.10108.
108. A. Stockdale, W. Davison and H. Zhang, *Earth-Sci. Rev.*, 2009, **92**, 81–97.
109. L. Pischedda, P. Cuny, J. L. Esteves, J.-C. Poggiale and F. Gilbert, *Hydrobiologia*, 2012, **680**, 109–124.
110. F. Wenzhöfer and R. N. Glud, *Limnol. Oceanogr.*, 2004, **49**, 1471–1481.
111. K. E. Brodersen, D. A. Nielsen, P. J. Ralph and M. Kühl, *New Phytol.*, 2015, **205**, 1264–1276.
112. P. N. Williams, J. Santner, M. Larsen, N. J. Lehto, E. Oburger, W. Wenzel, R. N. Glud, W. Davison and H. Zhang, *Environ. Sci. Technol.*, 2014, **48**, 8498–8506.
113. S. Jensen, M. Kühl, R. Glud, L. Jørgensen and A. Priemé, *Mar. Ecol.: Prog. Ser.*, 2005, **293**, 49–58.
114. C. R. Schroeder, G. Neurauter and I. Klimant, *Microchim. Acta*, 2007, **158**, 205–218.
115. C. Han, J. Ren, Z. Wang, H. Tang and D. Xu, *Water Res.*, 2017, **108**, 179–188.
116. N. J. Lehto, M. Larsen, H. Zhang, R. N. Glud and W. Davison, *Sci. Rep.*, 2017, **7**, 11369.
117. K. L. Michael, L. C. Taylor, S. L. Schultz and D. R. Walt, *Anal. Chem.*, 1998, **70**, 1242–1248.
118. J. A. Ferguson, B. G. Healey, K. S. Bronk, S. M. Barnard and D. R. Walt, *Anal. Chim. Acta*, 1997, **340**, 123–131.
119. S. M. Borisov, R. Seifner and I. Klimant, *Anal. Bioanal. Chem.*, 2011, **400**, 2463–2474.
120. D. B. Papkovsky and R. I. Dmitriev, *Chem. Soc. Rev.*, 2013, **42**, 8700–8732.

121. R. I. Dmitriev, A. V. Kondrashina, K. Koren, I. Klimant, A. V. Zhdanov, J. M. P. Pakan, K. W. McDermott and D. B. Papkovsky, *Biomater. Sci.*, 2014, **2**, 853.
122. R. I. Dmitriev, A. V. Zhdanov, G. Jasionek and D. B. Papkovsky, *Anal. Chem.*, 2012, **84**, 2930–2938.
123. R. N. Glud, H.-P. Grossart, M. Larsen, K. W. Tang, K. E. Arendt, S. Rysgaard, B. Thamdrup and T. Gissel Nielsen, *Limnol. Oceanogr.*, 2015, **60**, 2026–2036.